



Influence of additives on the Pt metal activity of naphtha reforming catalysts

Vanina A. Mazzieri, Javier M. Grau, Juan C. Yori, Carlos R. Vera, Carlos L. Pieck*

Instituto de Investigaciones en Catálisis y Petroquímica, INCAPE (FIQ-UNL, CONICET), Santiago del Estero 2654, S3000AOJ Santa Fe, Argentina

ARTICLE INFO

Article history:

Received 11 July 2008

Received in revised form 14 November 2008

Accepted 24 November 2008

Available online 6 December 2008

Keywords:

Naphtha reforming
Bimetallic catalysts

ABSTRACT

Alumina supported bimetallic Pt–Re, Pt–Sn and Pt–Ge naphtha reforming catalysts were studied. The Pt concentration was kept constant at 0.3% (weight basis) while the concentration of the second metal was varied in order to assess its influence. The experimental results showed that the addition of a second metal (Re, Sn, Ge) to the Pt catalyst produces a modification of the metal and acid functions. Sn and Ge produce similar modifications of the metal function: a marked decrease of the dehydrogenation and hydrogenolytic capacity of Pt. The addition of Re modifies the dehydrogenation capacity to a lower extent than the addition of Sn or Ge. The hydrogenolytic capacity is increased upon Re addition. The changes on the acid function are different depending on which metal is added. Re and Ge modify the acid strength distribution; they favor the formation of sites of lower acid strength but they keep the total concentration of acid sites almost constant. Conversely Sn addition not only produces a change in the acid strength distribution but also a decrease of the total acidity of the catalyst.

© 2008 Elsevier B.V. All rights reserved.

1. Introduction

The bifunctional metal–acid catalyst was introduced in the naphtha reforming process in 1949 [1,2]. Metal function properties were provided by Pt. The acid properties were supplied by the support itself that in this case was alumina promoted with chlorine. Since the original development many improvements have been introduced in the catalyst formulation but two features remain unaltered. The de/hydrogenation properties are mainly supplied by supported Pt particles and acid properties are supplied by the support itself. Modifications have consisted in the addition of promoters to the metal function, like Re, Sn or Ge [3–8], producing more selective and stable catalysts [9,10].

The oxidation state of Pt in the reduced Pt–Re/Al₂O₃ catalysts is currently accepted to be zero [11]. The oxidation state of Re is however still a matter of unresolved controversy. Some authors have failed to find zerovalent Re in commercial catalysts at reforming conditions [12] while others have found that Re is partly in the zerovalent state and partly as an oxide [13,14]. Some studies have finally revealed that Re would be totally reduced [15–17]. Metallic Re would join to Pt to form Pt–Re microcrystals, small atom groups or quasi-alloys known as “clusters” or “ensembles” [18]. These aggregates, which occur with pure Pt crystals, are very small in size and are very stable after they are formed on the surface of the alumina support.

More recently Pt–Sn/Al₂O₃ catalysts have received considerable attention. The conclusions about the chemical state of Sn are more consonance. It has been found that tin is partially alloyed with Pt [19,20], the remainder being ionic Sn(IV) and/or Sn(II) species [21–23]. Other modern catalysts are the Pt–Ge/Al₂O₃ ones. The oxidation state of Ge in these materials is not significantly affected by low temperature (i.e. 300 °C) reduction. At this temperature Pt is completely reduced but no Pt–Ge interactions can be observed. At higher temperatures (i.e. 500 °C), Ge cations located near Pt atoms or ensembles are reduced with the subsequent formation of Pt–Ge, alloy-like clusters [24].

Current theories about the modification of catalytic properties of Pt monometallic catalysts by addition of a second metal are based on electronic and/or geometrical considerations. The modification of Pt electronic properties leads to significant changes in adsorption energies of chemisorbed hydrocarbons so activity and selectivity are (favorably) affected. Such electronic modification has been attributed to an interaction between Pt and promoter oxide species [25] or to a direct alloy formation [26]. The improved resistance to catalyst deactivation by coking has been also attributed to electronic effects of this type [27–29].

On the other hand the main reactions of catalytic reforming have different structure sensitivity that depends on purely geometric factors. It is well known that de/hydrogenation reactions can proceed on simple (monoatomic) sites, but hydrogenolysis and coking require catalytic sites of a more complicated morphology (clusters or ensembles) [28–30]. The addition of a second inactive metal (Sn, Ge) to the catalyst places “spacers” between Pt groups and reduces the effective size of the

* Corresponding author. Tel.: +54 342 4533858; fax: +54 342 4531068.
E-mail address: pieck@fiq.unl.edu.ar (C.L. Pieck).

catalytically active Pt ensemble, hindering hydrogenolysis and coking processes and improving the catalyst performance. Pioneering works of Boudart on structure sensitivity [31,32] classified catalytic reactions as “demanding” (sensitive to morphological structure) and “facile” (structure-insensitive), according to the requirement or not of a particular ensemble of neighboring metal atoms in order to form adsorbate bonds with the proper strength. The geometric model has been recently refined as “ensemble-size” model [33–35] on the assumption that reaction rates are proportional to the probability of finding particular groups of neighboring atoms. Two classical test reactions are used that have an entirely different behavior according to the geometric factor theory: cyclopentane (CP) hydrogenolysis, which is a demanding one [36] and cyclohexane (CH) dehydrogenation which is non-demanding under the experimental conditions used. With the aid of these reaction tests the effect of the addition of a second metal to Pt can be assessed since both reactions are affected differently.

In this paper a systematic study using reaction tests is done in order to study the changes in the catalytic properties of Pt by addition of Ge, Re and Sn.

2. Experimental

2.1. Catalyst preparation

A commercial high-purity γ -alumina (Cyanamid Ketjen CK 300) was used as support. Main impurities were Na (5 ppm), Fe (150 ppm) and S (50 ppm). The extruded alumina pellets were ground and sieved and the 35–80 mesh fraction was separated and calcined in air (3 h at 650 °C). The specific surface area of this support was 180 m² g⁻¹, the pore volume 0.49 cm³ g⁻¹ and the average pore radius 5.4 nm. The metals were incorporated by coimpregnating the support with aqueous solutions of their corresponding salts. The amount and concentration of the solutions were adjusted in order to have a 0.3% of Pt and 0.1, 0.3, 0.9 and 2.0% of Ge (or Re or Sn) on the final catalyst. The precursors were H₂PtCl₆·6H₂O, NH₄ReO₄ and SnCl₂·2H₂O. The solution of the last precursor is unstable and was therefore prepared just before its use. The salt was first dissolved in deionised water and heated for 30 min at 70 °C. Then 37% HCl was added and the transparent solution was used.

Monometallic catalysts were also prepared. Al₂O₃ was immersed in a 0.2N HCl solution (1.5 ml g⁻¹) and then the necessary amount of the metal precursor solution was added. After 1 h under stirring at room temperature, the solvent was slowly evaporated by heating at 70 °C while stirring gently. The catalyst was then dried at 120 °C overnight, calcined in air (60 ml min⁻¹) for 4 h at 500 °C and then reduced in hydrogen (60 ml min⁻¹) for 4 h at 500 °C. Bimetallic catalysts were prepared following the same procedure used for monometallic catalysts.

The chloride content of the catalysts was determined by the Volhard–Charpentier method. The values were between 0.88 and 1.0% for all of them, a normal value for naphtha reforming catalysts due to the retention capacity of the support.

Because all the catalysts studied were supported on alumina, only the composition of this function is used to name the catalysts.

2.2. Temperature programmed reduction

TPR tests were performed in an Ohkura TP2002 apparatus equipped with a thermal conductivity detector. At the beginning of each TPR test the sample was heated in air at 450 °C for 1 h. Then it was heated from room temperature to 700 °C at a heating rate of 10 °C min⁻¹ in a reducing gas stream (5.0% H₂ in argon).

2.3. Dynamic chemisorption of CO

This technique was used to estimate the dispersion of the Pt metal particles on the surface of the catalyst. Calibrated pulses of the adsorbate were injected to a stream of inert gas that flowed over the sample. These pulses were sent to the reactor until the sample was saturated. At the beginning of the experiment the sample (400 mg) was reduced at 500 °C (10 °C min⁻¹) for 1 h. Then nitrogen was made to flow over the sample for 1 h at 500 °C in order to eliminate adsorbed hydrogen. Finally the sample was cooled down to room temperature in nitrogen and 0.6 μ mol of CO were sent to the reactor. Non-chemisorbed CO was quantitatively transformed into CH₄ over a Ni/Kieselguhr catalyst and detected in a flame ionization detector connected on-line. The error of the method was estimated by means of nine chemisorption tests with a Pt/Al₂O₃ catalyst with a dispersion of 40%. The average deviation was found to be of 4.3%.

2.4. CO-FTIR spectroscopy

FTIR spectra in the 4800–400 cm⁻¹ range were taken at room temperature in a Nicolet 5ZDX spectrometer with a resolution of 4 cm⁻¹. Self-supported wafers of the catalysts were first reduced at 500 °C under hydrogen flow for 30 min and then outgassed at 10⁻⁶ Torr at 500 °C for 30 min. Then the samples were contacted with 30 Torr of CO for 5 min and finally the samples were outgassed at 10⁻⁶ Torr at room temperature for 30 min and a spectrum was recorded.

2.5. Temperature programmed pyridine desorption

The quantity and amount of acid sites on the catalysts surface was assessed by means of temperature programmed desorption of pyridine. 200 mg of the catalyst were first immersed in a closed vial containing pure pyridine (Merck, 99.9%) for 4 h. Then the catalyst was taken out from the vial and excess pyridine was removed by evaporation at room temperature under a fume hood. The sample was then charged to a quartz microreactor and a constant nitrogen flow (40 cm³ min⁻¹) was established. Weakly adsorbed pyridine was first desorbed in a first stage of stabilization by heating the sample at 110 °C for 2 h. The temperature of the oven was then raised to 600 °C at a heating rate of 10 °C min⁻¹. The reactor outlet was directly connected to a flame ionization detector to measure the desorption rate of pyridine.

2.6. Cyclohexane dehydrogenation

The reaction was performed in a glass reactor with the following conditions: catalyst mass = 100 mg, temperature = 300 °C, pressure = 0.1 MPa, H₂ = 80 cm³ min⁻¹, cyclohexane = 1.61 cm³ h⁻¹. Before the reaction was started, the catalysts were treated in H₂ (80 cm³ min⁻¹, 500 °C, 1 h). The products were analyzed in a Varian 3400 CX chromatograph equipped with a FID and a packed column of FFAP on Chromosorb.

2.7. Cyclopentane hydrogenolysis

Before the reaction the catalysts were reduced for 1 h at 500 °C in H₂ (60 cm³ min⁻¹). Then they were cooled in H₂ to the reaction temperature (350 °C). The other conditions were: catalyst mass = 150 mg, pressure = 0.1 MPa, H₂ flow rate = 40 cm³ min⁻¹, cyclopentane flow rate = 0.483 cm³ h⁻¹. The reaction products were analyzed in a gas chromatograph connected on-line.

2.8. n-Pentane isomerization

It was carried out in a glass reactor, for 4 h, at 500 °C, 0.1 MPa, WHSV = 4.5 and molar ratio H₂:n-C₅ = 6. N-C₅ was supplied by

Merck (99.9%). The analysis of the reaction products was performed in a gas chromatograph connected on-line. Before the reaction, the catalysts were reduced at 500 °C for 1 h with hydrogen.

3. Results and discussion

Chemical analysis of catalysts by atomic absorption spectroscopy (AAS) showed metal contents were in close agreement with the expected theoretical ones for all samples.

3.1. Characterization by TPR

Temperature programmed reduction traces for bimetallic and monometallic catalysts are shown in Fig. 1. For the monometallic Pt catalysts a pronounced reduction peak at ca. 220 °C and a minor reduction band between 300 and 400 °C can be seen. This reduction pattern has been frequently observed by several authors [13,37–39] and it seems to be generally accepted that the first peak is due to the reduction of Pt oxide species weakly interacting with alumina. The less important second reduction band is assigned to the reduction of Pt oxochlorinated species in strong interaction with the support [9]. The monometallic Re catalyst has a unique, well defined reduction peak at about 590 °C. According to the measured hydrogen consumption, Pt species are completely reduced to Pt⁰ but Re oxides are only 90% reduced to metallic Re. For the bimetallic Pt–Re[0.1%] catalyst a broad reduction peak at ca. 450 °C can be seen that is attributed to the reduction of Re oxide species. The lower reduction temperature (as compared to the monometallic Re catalyst) can be explained by the catalytic effect of Pt on the reduction of Re oxides [40,41]. At a somewhat higher Re content (Pt–Re[0.3%] catalyst), such catalytic effect is more noticeable, leading to a more pronounced, lower temperature (ca. 350 °C) Re species reduction peak. For the Pt–Re[0.9%] catalyst the higher Re content leads to a broad reduction peak corresponding to the reduction of both Pt and Re species. This peak can be deconvoluted into two individual reduction peaks. Finally, at the highest Re content (2%), a pronounced reduction peak at ca. 315 °C can be observed (co-reduction of both metal oxide species). A higher temperature peak at 550 °C also appears that is due to the reduction of segregated Re oxide species [42–44].

The TPR trace of tin oxide is very broad. It begins at 150 °C and ends at 550 °C. Two bands can be seen at 200–300 °C and 380–520 °C. This behavior suggests an interaction between the Sn oxide and alumina leading to the formation of tin aluminates. According to some current literature [45] the Sn⁴⁺ species are reduced to Sn²⁺ ones due to a strong interaction with the support that impedes its further reduction to Sn⁰. Our results for hydrogen consumption indicate that about 80% of Sn⁴⁺ is reduced to Sn²⁺. For the bimetallic Pt–Sn catalysts a shift can be seen of the Pt reduction peak towards higher temperatures as Sn content increases. The reduction of Pt oxide is centered around 220 °C for Pt–Sn[0.1%] and at ca. 250 °C in the case of Pt–Sn[2.0%]. The appearance of a reduction peak at 300–400 °C as Sn content increases would correspond to the reduction of tin oxide species which could interact with Pt.

For the monometallic Ge catalyst a reduction peak at ca. 600 °C can be seen which corresponds to the reduction of Ge oxide species. The presence of Ge strongly influences the reduction of Pt. With a Ge content of only 0.1% the “normal” reduction peak at 220 °C is shifted up to 315 °C. At higher Ge loadings the reduction of Pt oxide species proceeds at higher temperatures and the size of the reduction peak corresponding to segregated Ge species (600 °C) increases. For the Pt–Ge [2.0%] catalyst the low temperature Pt reduction peak is no longer present. Two peaks, one at 580 °C and the other at 680 °C can be seen. The first one would correspond to the co-reduction of Pt and Ge oxide species. The second one would correspond to the reduction of segregated Ge species. Previous works on Pt–Ge catalysts reduced at 650 °C [46–48] concluded that germanium is present as Ge²⁺ and Ge⁰. Ge⁰ is alloyed to Pt. The shift of the reduction of Pt oxides to higher temperatures could be attributed to a hindering of the reduction of Pt species by a stronger interaction with Ge or to physical blocking [48].

3.2. Catalyst characterization by CO chemisorption

CO chemisorption data are presented in Fig. 2 as a function of the content of the second metal (Ge, Re, Sn). Previous results, not shown in this paper, indicated that at the experimental conditions used here the CO chemisorption on supported Ge, Re or Sn was not significant. It can be seen in this figure that the addition of Sn to Pt supported catalysts decreases its CO chemisorption capacity. These results are as expected because Sn has no capacity for chemisorb-

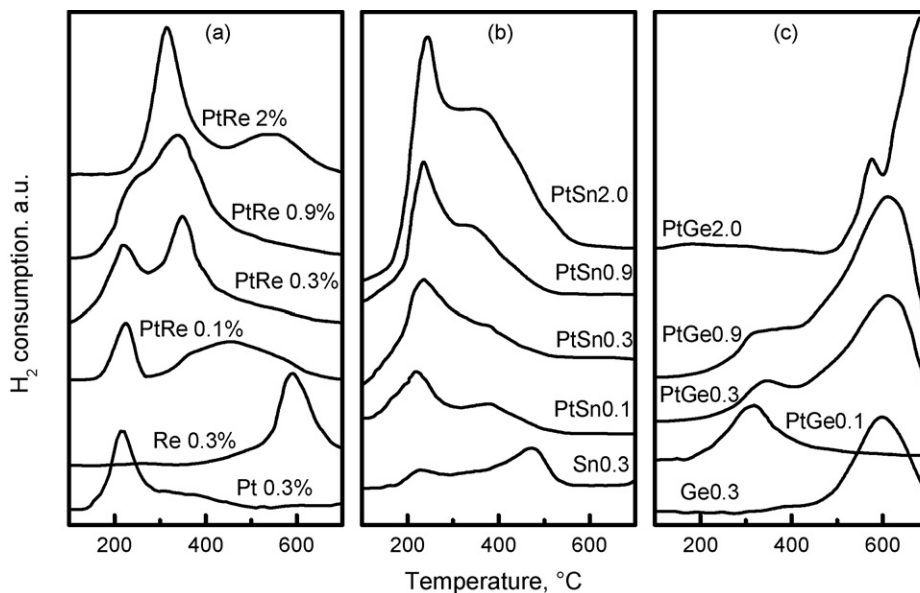


Fig. 1. TPR traces of bimetallic catalysts with different second metal loadings. Monometallic catalysts included as reference.

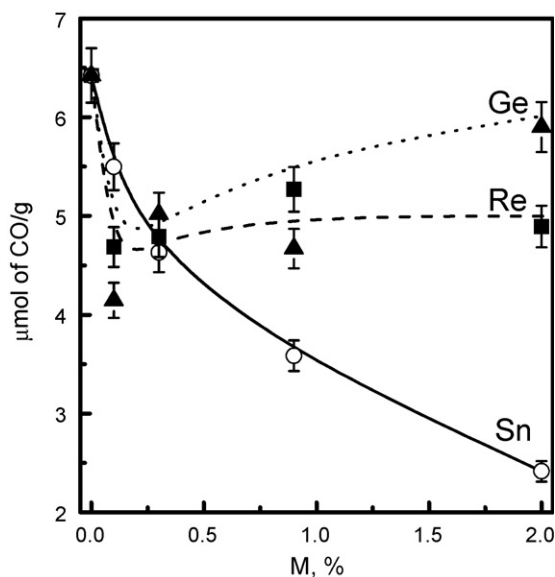


Fig. 2. Total CO uptake from chemisorption measurements as a function of second metal loading.

ing CO and its addition should decrease Pt CO chemisorption capacity. For the Pt–Re catalysts, the presence of Re also decreases the CO chemisorption capacity, but this effect seems to be mostly independent of its loading. A similar behavior of CO chemisorption for Pt–Ge catalysts can be observed, with an exception in the case of the highest Ge content, for which the chemisorption capacity increases. The atypical behavior of Pt–Re and Pt–Ge catalysts regarding CO chemisorption could be explained by a modification of the electronic structure of such metals due to the neighboring Pt atoms which could enhance its chemisorption capacity. Another possible explanation would be based in a Pt surface enrichment of Pt–Re and Pt–Ge clusters. Helfensteyn and Creemers [49] using Monte Carlo simulations combined with a “macroscopic atom” model investigated surface segregation in platinum–rhenium reforming catalysts and found that the surface of Re is richer in Pt. These results are in agreement with the considerably lower surface tension of Pt and the negative enthalpy of solution of the Pt–Re system [49]. Similar results were reported by Wang et al. [50]. Woosch et al. [51] found that adding 1–2 monolayers of Ge caused a new type of interaction in the sites containing both Pt and Ge. These sites adsorbed CO but did not adsorb hydrogen. A solid solution of Pt–Ge might have been formed thus creating “bulk bimetallic catalysts” with more surface Pt atoms not interacting with Ge.

3.3. FTIR spectra of chemisorbed CO

The FTIR spectra of monometallic Pt and bimetallic Pt–Re[0.3%], Pt–Ge[0.3%] and Pt–Sn[0.3%] catalysts are presented in Fig. 3. This technique is currently used to study surface metallic sites in reduced catalysts. CO molecules are adsorbed in linear or bridge configurations. The wavenumber range of Fig. 3 corresponds to the linear chemisorbed form that provides the most useful information to reveal electronic changes on the metal surface. The bridge absorption band, corresponding to CO–Pt₂ chemisorbed species, is usually weak so is not usually reported.

For the monometallic Pt catalysts a well defined absorption band can be seen at 2075 cm⁻¹, which corresponds to linear adsorption of CO on metallic Pt sites (CO–Pt⁰) [52]. Preliminary studies have shown that monometallic supported Re, Ge or Sn catalysts do not adsorb significant amounts of CO. Then absorption bands observed for bimetallic catalysts can be attributed to Pt

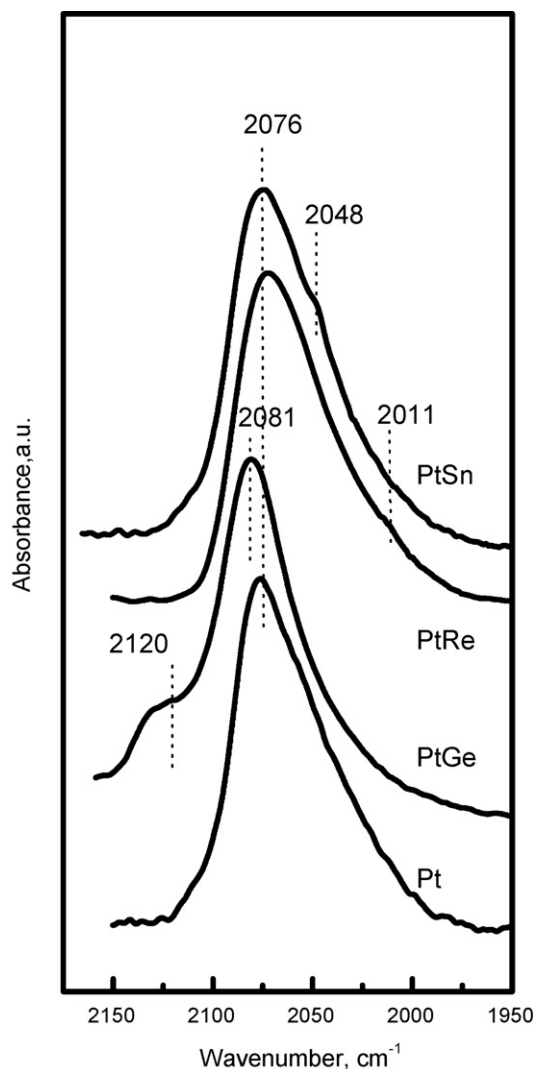


Fig. 3. FTIR absorption spectra of chemisorbed CO for monometallic Pt catalyst and bimetallic Pt–Ge[0.3%], Pt–Re[0.3%] and Pt–Sn[0.3%].

modified by the promoters. The IR spectrum for Pt–Re[0.3%] has a main absorption band corresponding to CO–Pt which is slightly shifted to lower frequencies (ca. 2073 cm⁻¹) and a small shoulder at 2011 cm⁻¹ possibly due to adsorption on Pt atoms influenced by electron transfer from neighboring Re atoms (CO–Pt^{δ-}) [9]. For Pt–Ge[0.3%] the maximum in the absorption band is shifted to higher frequencies (ca. 2081 cm⁻¹). This shift can be explained by considering that Ge acts as electron acceptor, lowering the electronic density of Pt [53]. An additional shoulder at 2120 cm⁻¹ can be observed which has been assigned to CO adsorbed onto Pt^{δ+} [54]. In the spectra of Pt–Sn[0.3%] catalyst there is a main absorption band at 2076 cm⁻¹, corresponding to CO adsorbed on metallic platinum, and a shoulder at 2048 cm⁻¹. According to the current bibliography the predominant alloy form of Pt–Sn has an 1:1 atomic ratio, and has an IR absorption band at 2048 cm⁻¹ [53–56] so this shoulder could correspond to electronically enriched Pt due to an electronic transfer from Sn. All these previously mentioned results clearly points to a modification of Pt electronic structure due to the presence of Sn, Ge or Re.

3.4. Characterization by pyridine TPD

The TPD experiments showed that the addition of Ge causes desorption peaks shifts towards lower temperatures, suggesting

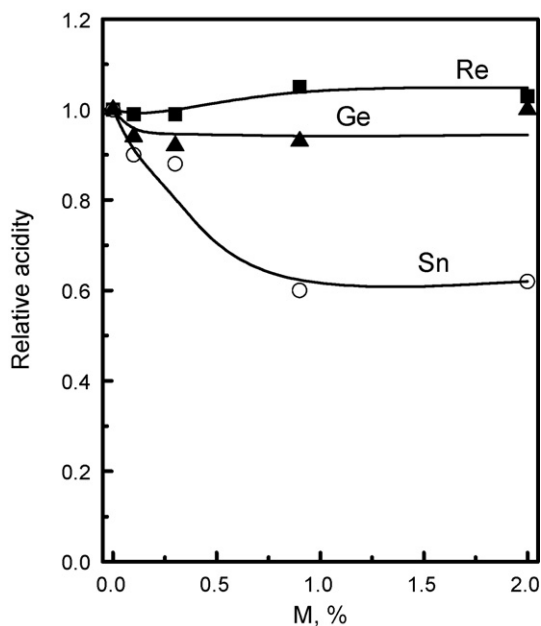


Fig. 4. Relative acidity (from pyridine TPD) for the bimetallic catalysts as a function of second metal loading.

that weak acid sites are created or strong sites are destroyed. The same behavior was observed upon incorporation of Re to the Pt catalyst (results not shown). This can be explained by the weak acid nature of both Ge and Re oxides which might displace chlorine from the alumina surface. It is well known that the addition of chlorine creates strong acid sites on the alumina surface [57,58]. In Fig. 4 the variation of total acidity upon the addition of the promoters can be seen. The incorporation of Sn markedly diminishes the total acidity, but this parameter is much less affected in the case of Ge or Re addition. The marked effect of Sn addition is attributed to the basic nature of Sn oxides which can partly neutralize the acidity of the chlorinated support. These results are in agreement with previous findings of Carvalho et al. [10,9] about the effect of Sn and Re addition on the acidity of Pt catalysts. Regarding the effect of Ge on acidity, Galisteo et al. [59] found an increase in catalysts acidity. Conversely de Miguel et al. [47] found no modification of the acidity as measured by ammonia TPD.

3.5. Test reactions

3.5.1. Cyclohexane dehydrogenation

Relative conversions for this reaction taking the monometallic Pt catalyst as a reference are shown in Fig. 5 as a function of the promoter loading. All points are mean values from the averaging of 12 consecutive measurements equally spaced along the whole run. No significant catalyst deactivation was observed in any run. The presence of Sn, Ge or Re has a negative effect on the catalyst activity as seen in Fig. 5. The effect of Re is less pronounced. A 20% decrease in activity is observed for the highest Re loading (Pt–Re[2%] catalyst). The addition of Sn and Ge has a profound negative effect on the catalytic activity for this reaction. The relative activity drops to only 1% upon addition of 0.9% Ge or Sn, and for the highest second metal loadings there is not any activity at all.

The dehydrogenation of cyclohexane is a typical metal-catalyzed, non-demanding reaction (it does not require the presence of particular atom ensembles) [31]. Additional runs with the monometallic Re, Ge and Sn catalysts showed that the relative conversion was only 0.06 for Re and that almost no activity could be measured for Ge or Sn catalysts. It therefore seems that the non-

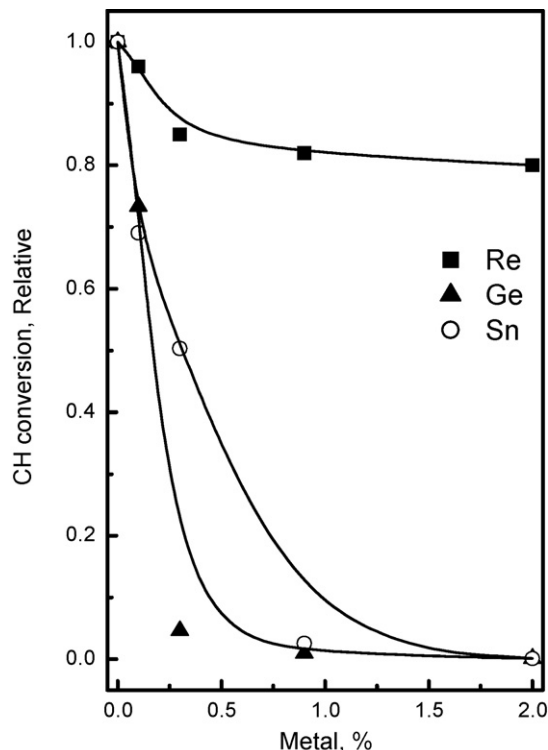


Fig. 5. Relative conversion of cyclohexane for the bimetallic catalysts as a function of second metal loading.

linear diminution of activity with the increase in the second metal loading could be explained assuming that: (i) the distribution of the second metal in the metal phase is selective (i.e. non-uniform), or (ii) the non-demanding reaction model does not operate. As mentioned before the TPR results revealed a strong interaction between Pt and the second metal, and that for the Pt–Ge catalyst with the highest Ge loading the reduction of Pt was markedly retarded possibly due to a covering effect of Ge atoms. These facts could explain the non-linear decrease of the activity. The modest modification of activity upon Re addition was rather unexpected because other experimental results indicated a strong Pt–Re interaction. Moreover Re has a low intrinsic activity in dehydrogenation. An explanation of this “unusual” behavior could be found in the observed formation of Pt–Re alloys with a Pt-enriched surface [26,44]. A comparison of the changes in CO chemisorption capacity (Fig. 2) with the variation of activity for this reaction (Fig. 5) unveils a close similarity in their patterns. It follows, as previously mentioned, that the metallic activity of the Pt–Sn catalyst can be predicted from CO chemisorption measurements. In contrast for the Pt–Ge catalyst CO chemisorption and cyclohexane dehydrogenation data have no matching patterns. CO chemisorption seems to be independent of Ge loading while conversely metallic activity is strongly influenced. This could be due to the different amount of Pt atoms needed for CO chemisorption and CH dehydrogenation. These are one and two, respectively. Ge addition would increase the concentration of 1-atom Pt species thus inhibiting CH dehydrogenation while CO chemisorption is unaltered. Another possible explanation is that electronic modifications imposed by Ge alter the activation energy of each reaction differently. CH dehydrogenation is thus highly inhibited while CO chemisorption is not.

3.5.2. Cyclopentane hydrogenolysis

Results obtained in this test reaction for the bimetallic catalysts are shown in Fig. 6 as a function of the second metal loading. As

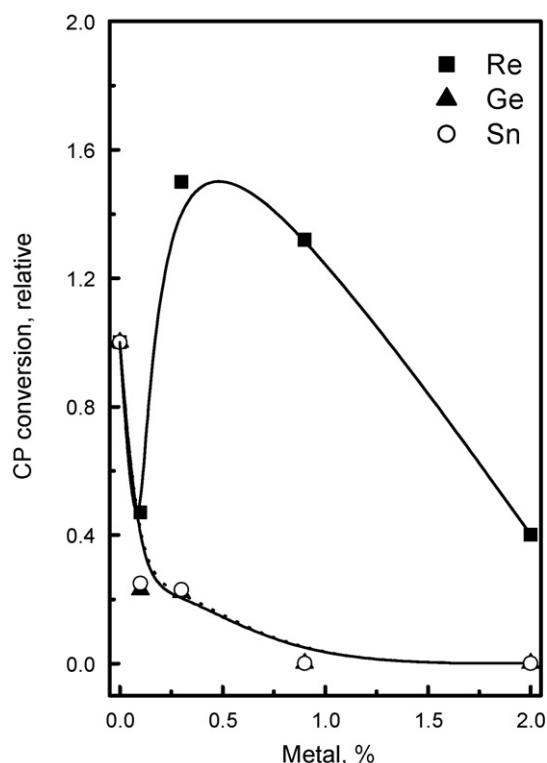


Fig. 6. Relative conversion of cyclopentane for the bimetallic catalysts as a function of second metal loading.

catalysts rapidly deactivate by coking in this reaction all results correspond to 5 min time-on-stream for comparative purposes. A marked negative effect on catalyst activity when Ge or Sn is added can be clearly seen. This effect has the same magnitude for both metals (experimental points are practically the same for each metal loading). These results are easily understood by considering the demanding character of cyclopentane dehydrogenation reaction [56]. Small additions of Ge or Sn (both practically inactive in the experimental conditions used) profoundly affect the catalytic activity. This effect could be due to geometric or electronic factors operating on metallic Pt. The geometric factor involves the blocking of active Pt ensembles by added promoter atoms. The electronic factor corresponds to the modification of the Pt electronic density due to an interaction with Ge or Re neighboring atoms. Such electronic modification would in turn change the energy of adsorption of the chemical species participating in the catalytic reaction. It has been proved that both effects are important [60,61].

In the case of the Pt–Re catalysts an initial activity drop can be seen upon Re addition (0.1% Re). Further Re additions increase the activity. This reaches a maximum and then decreases again upon further Re loading. A similar behavior has previously been reported for Pt–Re catalysts prepared by catalytic reduction [26,62]. There exists a synergistic effect between Pt and Re for this hydrogenolytic reaction. This could be due to the importance of the adsorption energy of hydrogenolysis precursor species as decisive parameters in the formation of the complex leading to the rupture of C–C bonds. Pt ensembles have low adsorption heat for these species, and the opposite (i.e. high adsorption energy) is true for pure Re [63]. Intermediate values for adsorption heats are found for Pt–Re ensembles. The hydrogenolytic activity can therefore be taken as an indirect measurement of Pt–Re interaction [63] as Pt–Re ensembles are more active than Pt or Re alone.

It is interesting to compare the behavior of Pt–Sn and Pt–Ge catalysts on both reactions (cyclohexane dehydrogenation and

cyclopentane hydrogenolysis). According to the current theory of demanding and non-demanding reactions, the hydrogenolytic activity should be much more affected than the dehydrogenating one. A similar decrease in activity for both reactions is nevertheless observed at the highest ($\geq 0.9\%$) Ge or Sn loading. This unexpected results could be due to the very low metallic activity as a consequence of Pt blocking by “inert” Ge or Sn atoms. In any case a marked difference between hydrogenolytic activity and hydrogenating activity should be measured.

These anomalous results could be explained by considering that active sites on monometallic Pt catalyst and bimetallic Pt–Sn or Pt–Ge catalysts are not equivalent due to the presence of electronic (metals interaction) effects which render the demanding–non-demanding concept not applicable. The addition of the second metal would profoundly modify the electronic properties of Pt which are responsible of its catalytic activity. Such modifications would be more important as the second metal loading increases, making the use of monometallic Pt catalyst as a reference not appropriate.

The experimental results showed that the effect of the addition of a second metal mainly depend on the nature of the metal itself. As Sn and Ge are considered as catalytically inactive elements, it should be expected that they would modify the metal function in the same way. However the results obtained from chemisorption, dehydrogenation and hydrogenolysis clearly show noticeable differences. Such differences are more profound in the case of Re (which is considered a catalytically active element). All these results indicate that electronic (interaction) effects are very important and relatively more relevant than geometric ones. Some further information on the electronic effect can be obtained by calculating the activation energy of the CH dehydrogenation reaction, as was reported in a previous paper [9]. This was done by performing the test at different temperatures (300, 325, 375 and 400 °C) and assuming a first-order reaction. The activation energy value of Pt–Re was similar to the value of Pt (20 kcal/mol), revealing a small modification of the active sites of Pt by Re. The activation energy of Pt–Sn was higher than the activation energy of Pt (26–34 kcal/mol, depending on the order of impregnation of Pt and Sn [9]). It is important to remark that the Pt–Sn values depend on the impregnation order because the magnitude of the Pt–Sn interaction is a function of this order.

3.5.3. *n*-Pentane reforming

The catalytic transformation of *n*-pentane on dual function (metal/acid) catalysts yields many products: 1, isopentane, as a consequence of the bifunctional, acid controlled, isomerization reaction; 2, lighter gaseous hydrocarbons (C_2 and C_3) from cracking reactions partly controlled by the metal function and partly by the acidic function; 3, cyclopentane by dehydrocyclization on metal sites and 4, methane from hydrogenolysis on the metallic sites.

No aromatic compounds can be formed from nC_5 reforming so the main products are paraffin isomers. It is currently accepted that the C_5 isomerization mechanism is a bifunctional (metal–acid) one [64]. The linear paraffin is firstly dehydrogenated on metallic sites, the produced olefin being then isomerized on acid sites. This olefin isomer is finally re-hydrogenated on the metallic site and the isoparaffin is obtained. The rate controlling step of this mechanism is the acid catalyzed one [65] so the formation of *i*-pentane can be taken as a measure of this catalytic function. It has been nevertheless reported that a monofunctional metal-catalyzed mechanism for isomerization may take place through the hydrogenolysis of five carbon atoms rings [60,64], but its contribution at the experimental conditions used here seems to be negligible [60].

In Fig. 7 values of the initial (5 min time-on-stream) total *n*-pentane conversion and of the relative deactivation parameter

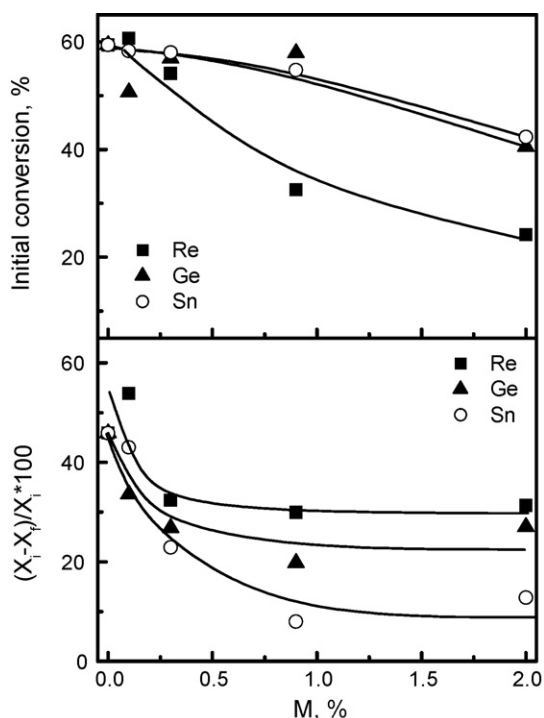


Fig. 7. Values of the initial (5 min time-on-stream) total n-pentane conversion and of the relative deactivation parameter ($\chi = (x_{5 \text{ min}} - x_{240 \text{ min}})/x_{5 \text{ min}}$) as a function of the second metal content.

($\chi = (x_{5 \text{ min}} - x_{240 \text{ min}})/x_{5 \text{ min}}$) were plotted as a function of the second metal content. Big χ values indicate a great degree of deactivation of the catalyst. Except Pt–Re[0.1%] all catalysts have a lower initial activity than the monometallic Pt catalyst. When the concentration of the second metal is increased the initial conversion is decreased. Pt–Ge and Pt–Sn have a greater initial conversion than Pt–Re. All catalysts are more stable (lower χ) than monometallic Pt. It can be seen that second metal contents as high as 0.3% increase the stability but this effect fades away at higher contents. Stability follows the order: Pt–Sn > Pt–Ge > Pt–Re. The lower initial conversion of bimetallic Pt–Re, Pt–Ge and Pt–Sn with respect to monometallic Pt can be explained by the inhibiting effect of the second metal on both the metal and acid functions. The hydrogenolytic and dehydrogenating metal activities are decreased and the same happens with the strong and overall acidity.

The increased catalyst stability upon Ge or Sn addition is easily understood taken into account the associated decrease in Pt dehydrogenating capacity, leading to a lower formation of dehydrogenated species acting as coke precursors [66,67]. The addition of any of the two metals also causes a decrease in the amount of strong acid sites responsible for polymerization reactions that lead to coke formation. The better stability of Pt–Re catalysts as compared with the monometallic Pt catalyst could be due to the fact that Re addition does not greatly modifies its dehydrogenating capacity. The amount of coke precursors would not be therefore substantially changed. But the higher hydrogenolytic capacity of Pt–Re catalysts would lead to a more efficient elimination of such coke precursors thus improving the stability with respect to the Pt catalyst.

Selectivities to C₅ isomers, C₁/C₃ ratios and coke contents are shown in Table 1. In agreement to results reported in Fig. 7, the addition of the second metal produces a lower coke deposition; the higher the second metal concentration the lower the final coke content. This behavior was attributed to the lower acidity of the promoted catalysts and the poorer dehydrogenating capacity of

Table 1

i-C₅ selectivities, C₁/C₃ ratios and carbon percentage (as determined by TPO) at end of run (240 min). Influence of second metal loading.

Catalysts (% second metal)	Re			Ge			Sn		
	SiC ₅	C ₁ /C ₃	C, %	SiC ₅	C ₁ /C ₃	C, %	SiC ₅	C ₁ /C ₃	C, %
0.0	20.2	0.51	0.59	20.2	0.51	0.59	20.2	0.51	0.59
0.1	25.8	0.57	0.58	23.2	0.45	0.30	47.4	0.10	0.29
0.3	23.2	0.72	0.34	47.0	0.18	0.28	61.2	0.10	0.22
0.9	26.8	0.89	0.28	51.4	0.13	0.28	63.0	0.12	0.06
2.0	11.9	2.47	0.24	43.4	0.13	0.24	48.3	0.12	0.01

SiC₅: selectivity to C₅ isomers, %, C: carbon percentage obtained by TPO.

the Pt–Sn and Pt–Ge catalysts, and in the case of Pt–Re catalysts, the destruction of the coke precursors by hydrogenolysis.

An improvement in the selectivity to C₅ isomers upon the addition of the second metal can also be seen, being this effect more noticeable for the Pt–Sn[0.9%] catalyst. The increase in selectivity to branched isomers observed on bimetallic catalysts can be explained by the acid site control theory. Results from pyridine TPD experiences revealed a decrease of strong acid sites and the creation of weak ones in bimetallic catalysts. A negative effect on hydrocracking is expected because these reactions require strong acid sites while a positive effect on isomerization is expected because this occurs on milder acid sites. On the other hand, both Sn or Ge addition adversely affects the Pt metal function so a decrease in hydrogenolysis products and an increase in selectivity to isomers is moreover expected. Methane is a typical product of hydrogenolysis on Pt metal sites [61], which is a demanding reaction [56], and its formation rate is higher for the monometallic Pt catalyst than for the bimetallic Pt–Sn and Pt–Ge catalysts. Such lower hydrogenolytic activity of these bimetallic catalysts can be understood taking into account the disappearance of Pt atom ensembles by the incorporation of the second metal atoms [33,68]. These results are in agreement with those reported about hydrogenolytic activity in Fig. 6. For the bimetallic Pt–Re catalysts, the higher hydrogenolytic activity (i.e. methane production) could be due to a synergistic effect between the two metals. Results for hydrogenolytic activity in this case are again in agreement with those reported in Fig. 6. Higher C₁/C₃ ratios are observed in Pt–Re catalysts in comparison to Pt, Pt–Ge or Pt–Sn. The lower isomer yields obtained for Pt–Re catalysts could then naturally arise from the hydrogenolytic destruction of the intermediate olefins in the isomerization mechanism.

The values of the C₁/C₃ ratio in Table 1 are a measure of the relative (hydrogenolysis/hydrocracking) activities. The results are dominated by the variation in the hydrogenolytic activity as modified by the second metal. Re addition increases the C₁/C₃ ratio due to the higher intrinsic hydrogenolytic activity of Pt–Re. Conversely Sn and Ge addition decrease the activity of the base metal, Pt.

4. Conclusions

Experimental results show that the addition of a second metal (Re, Sn, Ge) to monometallic Pt/Al₂O₃ catalysts modifies both the metal and acid functions.

The modifications imposed by Sn or Ge addition are similar: a pronounced decrease in the original hydrogenolytic/dehydrogenating capacity of Pt monometallic catalyst. The linear correlation between CO chemisorption capacity and dehydrogenating activity observed for Pt–Sn catalysts is nevertheless not observed for Pt–Ge catalysts. The addition of Re modifies the dehydrogenating activity of Pt in a much lesser extent than Ge or Sn, but a noticeable increase in hydrogenolytic activity is observed.

The modification of the acidic function due to the addition of the second metal depends on the nature of the added metal. The incorporation of Re or Ge does not greatly affect the value of total acidity but shifts the distribution towards weaker sites. The addition of Sn not only changes the acid strength distribution but also decreases the total acidity.

The n-pentane reforming results confirm the previous trends. The addition of the second metal negatively affects the original Pt metal function, decreasing the formation of dehydrogenated species (coke precursors), and also inhibiting polymerization and coke forming via a decrease of the average acid strength. The selectivity to isomers is increased.

References

- [1] V. Hansel, U.S. Patents 2,479,101, UOP, 1949.
- [2] V. Hansel, U.S. Patents 2,479,110, UOP, 1949.
- [3] J.H. Sinfelt, US Patent 3,415,737, 1979.
- [4] A.C. Muller, P.A. Engelhard, J.E. Wiesang, *J. Catal.* 56 (1975) 65.
- [5] R. Bouwman, P. Biloen, *J. Catal.* 48 (1979) 209.
- [6] H.E. Kluskdahl, U.S. Patent 3,415,737, UOP, 1968.
- [7] R.E. Rausch, US Patent 3,745,112, UOP, 1975.
- [8] K.R. McCallister, T.P. O'Neal, French Patent 2,078,056, UOP, 1971.
- [9] L.S. Carvalho, C.L. Pieck, M.C. Rangel, N.S. Figoli, J.M. Grau, P. Reyes, J.M. Parera, *Appl. Catal. A* 269 (2004) 91.
- [10] L.S. Carvalho, C.L. Pieck, M.C. Rangel, N.S. Figoli, C.R. Vera, J.M. Parera, *Appl. Catal. A* 269 (2004) 105.
- [11] J. Xiao, R.J. Puddephatt, *Coord. Chem. Rev.* 143 (1995) 457.
- [12] M.F.L. Johnson, V.M. Leroy, *J. Catal.* 35 (1974) 434.
- [13] S.M. Augustine, W.M.H. Sachtler, *J. Catal.* 116 (1989) 184.
- [14] N.S. Nacheff, L.S. Kraus, M. Ichikawa, B.M. Hoffman, J.B. Butt, W.M.H. Sachtler, *J. Catal.* 106 (1987) 263.
- [15] N. Wagstaff, R. Prins, *J. Catal.* 59 (1979) 434.
- [16] B.D. Mc Nicol, *J. Catal.* 46 (1977) 438.
- [17] A.N. Webb, *J. Catal.* 39 (1975) 485.
- [18] J.H. Sinfelt, in: J.R. Anderson, M. Boudart (Eds.), *Catalysts—Science and Technology*, Springer-Verlag, Berlin, Heidelberg, New York, 1981 (Chap. 5).
- [19] R. Bicaud, P. Bussière, F. Figueras, *J. Catal.* 69 (1981) 399.
- [20] Y. Li, K.J. Klabunde, B.H. Davis, *J. Catal.* 128 (1991) 1.
- [21] V.I. Kuznetsov, A.S. Belyi, E.N. Yurchenko, M.D. Smolikov, M.T. Protasova, E.V. Zatulokina, V.K. Duplyakin, *J. Catal.* 99 (1986) 159.
- [22] C.S. Vertes, E. Talas, I. Czako-Nagy, J. Ryczkowski, S. Göbölös, A. Vertes, J. Margitfalvi, *Appl. Catal.* 68 (1991) 149.
- [23] M.C. Hobson, S.L. Goresch, G.P. Khare, *J. Catal.* 142 (1993) 641.
- [24] A. Borgna, T.F. Garetto, C.R. Apesteguía, B. Moraweck, *Appl. Catal. A* 182 (1999) 189.
- [25] R. Burch, L.C. Garla, *J. Catal.* 71 (1981) 360.
- [26] C. Betizeau, G. Lerercq, R. Maurel, C. Bolivar, H. Charcosset, L. Tournayan, *J. Catal.* 45 (1976) 179.
- [27] R.J. Burch, *J. Catal.* 71 (1981) 348.
- [28] B. Coq, F. Figueras, *J. Catal.* 85 (1984) 197.
- [29] F.H. Ribeiro, A.L. Bonivardi, C. Kim, G.A. Somorjai, *J. Catal.* 150 (1994) 186.
- [30] P. Biloen, F.M. Duatzenberg, W.M.H. Sachtler, *J. Catal.* 50 (1977) 77.
- [31] M. Boudart, A. Aldag, J.E. Benson, V.A. Dougharty, C.G. Harkings, *J. Catal.* 6 (1966) 92.
- [32] M. Boudart, in: *Proceedings of the 6th International Congress of Catalysis*, The Chemical Society, London, (1976), p. 1.
- [33] W.M.H. Sachtler, R.A. van Santen, *Adv. Catal.* 26 (1977) 69.
- [34] R. Coekelbergs, A. Frennet, G. Lienard, P. Resibois, *J. Phys. Chem.* 39 (1963) 604.
- [35] J.A. Dalmon, G.A. Martin, *J. Catal.* 66 (1980) 214.
- [36] F.G. Gault, *Adv. Catal.* 30 (1981) 1.
- [37] H. Lieske, G. Lietz, H. Spindler, J. Völter, *J. Catal.* 81 (1983) 8.
- [38] G. Lietz, H. Lieske, H. Spindler, W. Hanke, J. Völter, *J. Catal.* 81 (1983) 17.
- [39] T.F. Garetto, A. Borgna, E. Benvenuto, C.R. Apesteguía, *XII Simp. Iberoam. Catal.*, 1990, p. p585.
- [40] B.H. Isaac, E.E. Petersen, *J. Catal.* 85 (1984) 8.
- [41] L. Chen, Y. Li, J. Zang, H. Luo, S. Cheng, *J. Catal.* 145 (1994) 132.
- [42] C.L. Pieck, M.B. González, J.M. Parera, *Appl. Catal. A* 205 (2001) 305.
- [43] V. Benitez, M. Boutzeloit, V.A. Mazzieri, C. Especel, F. Epron, C.R. Vera, P. Marécot, C.L. Pieck, *Appl. Catal. A* 319 (2007) 210.
- [44] R. Prestivik, K. Moljord, K. Grande, A. Holmen, *J. Catal.* 174 (1998) 119.
- [45] R. Bicaud, O. Bussiere, F. Figueras, M. Mathieu, *C.R. Acad. Sci. Paris Ser. C* 281 (1975) 159.
- [46] S.R. de Miguel, O.A. Scelza, A.A. Castro, *Appl. Catal.* 44 (1988) 23.
- [47] S.R. de Miguel, J.A. Martinez Correa, G.T. Baronetti, A.A. Castro, O.A. Scelza, *Appl. Catal.* 60 (1990) 47.
- [48] M.C. Souza Santos, J.M. Grau, C.L. Pieck, J.M. Parera, J.L.G. Fierro, N.S. Figoli, M.C. Rangel, *Catal. Lett.* 103 (3–4) (2005) 229.
- [49] S. Helfensteyn, C. Creemers, *Surf. Sci.* 78 (2002) 507.
- [50] G. Wang, M.A. Van Hove, P.N. Ross, M.I. Baskes, *J. Chem. Phys.* 121 (2004) 5410.
- [51] A. Wootsch, Z. Paál, N. Györfy, S. Eilo, I. Boghian, J. Leverd, L. Pirault-Roy, *J. Catal.* 238 (2006) 67.
- [52] M.G.V. Mordente, C.H. Rochester, *J. Chem. Soc. Faraday Trans. I* 85 (1989) 3045.
- [53] N. Macleod, J.R. Fryer, D. Stirling, G. Bebb, *Catal. Today* 46 (1998) 37.
- [54] A.V. Ivanov, A. Yu Stakheev, L.M. Kustov, *Russ. Chem. Bull.* 47 (1999) 1255.
- [55] J. Volter, H. Lieske, G. Lietz, *React. Kinet. Catal. Lett.* 16 (1981) 87.
- [56] G.A. Mills, H. Heinemann, T.H. Milleken, A.G. Oblad, *Ind. Eng. Chem.* 45 (1953) 134.
- [57] A. Ayame, G. Sawada, H. Sato, G. Zhang, T. Ohta, T. Izumizawa, *Appl. Catal.* 48 (1989) 25.
- [58] M. Tanaka, S. Ogasawara, *J. Catal.* 16 (1957) 157.
- [59] F.C. Galisteo, R. Mariscal, J.L.G. Fierro, G. Collins, J.C. Yori, J.M. Parera, J.M. Grau, *XIX Simp. Iberoam. Catal.* (2004) 3205.
- [60] J.M. Parera, N.S. Figoli, in: G.J. Antos, A.M. Aitani, J.M. Parera (Eds.), *Catalytic Naptha Reforming: Science and Technology*, Marcel Dekker Inc., New York, 1995 (Chap. 3).
- [61] M.D. Edgar, in: B.E. Leach (Ed.), *Applied Industrial Catalysis*, vol. 1, Academic Press, New York, 1983, p. 123.
- [62] C.L. Pieck, P. Marécot, J.M. Parera, J. Barbier, *Appl. Catal. A* 126 (1995) 153.
- [63] S.M. Augustine, W.M.H. Sachtler, *J. Catal.* 116 (1989) 184.
- [64] C.A. Querini, N.S. Figoli, J.M. Parera, *Appl. Catal.* 52 (1989) 249.
- [65] D.E. Sparks, R. Srinivasan, B.H. Davis, *J. Mol. Catal.* 88 (1994) 359.
- [66] C. Kappenstein, M. Saouabe, M. Guérom, P. Marécot, I. Uszkurat, Z. Paál, *Catal. Lett.* 31 (1995) 9.
- [67] A. Borgna, T.F. Garetto, C.R. Apesteguía, *Appl. Catal. A* 197 (2000) 11.
- [68] F.M. Dautzenberg, J.N. Helle, P. Biloen, W.M.H. Sachtler, *J. Catal.* 63 (1980) 571.